13A.3 VALIDATION OF A THEORETICAL MODEL FOR LARGE TURBINE ARRAY PERFORMANCE UNDER REALISTIC ATMOSPHERIC CONDITIONS

Thomas D Dunstan*
UK Met Office, Exeter, UK
Toshimitsu Murai
Cranfield University, UK
Takafumi Nishino
Cranfield University, UK

1. INTRODUCTION

Theoretical models capable of describing the performance of wind turbine arrays can be used to explore a wide range of parameters and to guide the design of more expensive and detailed numerical experiments. However their validity under realistic atmospheric conditions must first be established. In this study we aim to test one such theoretical model (Nishino, 2016, henceforth N16) under realistic forcing conditions, to attempt to identify the circumstances under which it succeeds, and also where it begins to loose accuracy, and suggest some possible reasons why this might occur.

2. TWO-SCALE MOMENTUM THEORY

The N16 model used in this study is based on two-scale coupled momentum analysis. In the following, subscript 0 denotes conditions before construction of a wind farm.

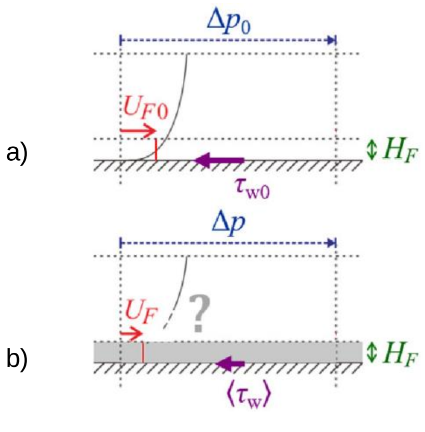

Fig. 1. Schematic of the two-scale momentum analysis where a) and b) depict conditions before and after farm construction respectively. From Nishino (2018).

* tom.dunstan@metoffice.gov.uk

A momentum balance is considered at the scale of individual turbines using classical actuator disk theory (e.g. Hansen, 2015), and coupled with a momentum balance across the larger scale wind farm layer. Details of the derivation can be found in Nishino (2016). The final form of the model can be expressed:

$$4\alpha(1-\alpha)\frac{\lambda}{C_{f0}}\beta^2+\beta^\gamma-1=0 \qquad (1)$$

where $1-\alpha = 1-(U_T/U_F)$ is a local induction factor, U_T is the average streamwise velocity across each turbine, and U_F is the average wind farm layer velocity. $\lambda = A/S$ is the array density where A is the rotor swept area and S is the horizontal area associated with each turbine, C_{f0} is the non-dimensional 'natural' surface friction coefficient of the site before farm construction, and $\beta = U_F/U_{F0}$ indicates how much the farm layer wind speed has decreased from its pre-construction state. The exponent γ is a free parameter to be determined empirically.

A key concept in the definitions of α and β is the identification of a nominal farm layer height, H_F, as illustrated in Fig. 1. This is defined from the natural wind profile:

$$U_{F0} = \frac{\int_0^{H_F} U_0 dz}{H_F} = \frac{\int U_0 dA}{A} \qquad (2)$$

Using Eq. 1 to relate α and β for a given set of λ, C_{f0}, and γ, two power coefficients can be defined:

$$C_p = \frac{TU_T}{\rho U_{F0}^3 A/2} = 4\alpha^2(1-\alpha)\beta^3 \qquad (3)$$

$$C_p^* = \frac{TU_T}{\rho U_F^3 A/2} = 4\alpha^2(1-\alpha) \qquad (4)$$

Similarly, a local thrust coefficient can be defined:

$$C_T' = \frac{T}{\rho U_T^2 A/2} = 4(1-\alpha)/\alpha \qquad (5)$$

The validity of Eq. 1 has been tested in various idealised settings (Ghaisas 2017, Zapata 2017, Nishino 2016), and found to perform well, with differences in the range 5%-20% and 1%-10% for C_P and C_T respectively compared to 3D numerical simulations. In situations where direct wake interactions are important it has a tendency to overpredict the available turbine power, since the actuator disk model does not explicitly take this into account. Equation 1 also assumes that the pressure gradient remains unchanged after construction of the wind farm ($\Delta P_0 = \Delta P$), however an extension to Eq. 1 has recently been proposed (Nishino, 2018) which relaxes this assumption with the addition of a simple correction term to the RHS:

$$(\Delta P - \Delta P_0)/\Delta P_0 \qquad (6)$$

However, in this study only Eq. 1 is used.

3. LARGE-EDDY SIMULATIONS

Simulations were carried out using the Met Office – NERC Cloud Model (MONC), (Brown, 2017). Individual turbines were represented as momentum sinks following the actuator disk model described in Calaf (2010). The domain is horizontally periodic and uses a solid lid with a damping layer to prevent spurious reflections. Domain and turbine parameters are given in Table 1. The configuration was chosen to allow direct comparison with cases A1 and A2 in Calaf (2010).

Turbine hub height (m)	100
Turbine rotor diameter (m)	100
Surface roughness length, z0 (m)	10^{-4}
Domain dimensions x,y,z (km)	π x π x 1
Grid size x, y, z	128^3
C_T'	1.33
Turbine configuration	4 x 6

Table 1. Simulation parameters

Realistic forcing profiles used to initialise and drive the simulations were extracted from the Met Office's UKV 1.5km local area model, which is used operationally to provide high resolution forecasts over the British Isles. Sample profiles were taken from a location in the North Sea off the east coast of Scotland. Instantaneous vertical profiles of u, v and θ were extracted at the shortest possible lead times, then averaged over a 3 hour window to remove small scale variations and provide quasi-steady conditions. The large eddy simulations were then forced towards these profiles using Newtonian relaxation with relaxation period, T_R . In addition, a uniform forcing profile (u = 10ms^{-1}) was also simulated. Note that the use of relaxation forcing is necessary in order to reproduce the desired boundary layer profiles but it is not directly compatible with the assumption of a constant pressure gradient used in Eq. 1. Simulations were repeated using three values of T_R (1800s, 3600s, and 7200s) to test the sensitivity of the results to this parameter. In addition, to compensate for the fact that $\Delta P \neq \Delta P_0$ a correction is required in the calculation of U_{F0} and the surface shear stress τ_{w0} as detailed in Section 4.

Forcing profiles were categorised as stable, unstable or neutral based on the bulk Richardson number, and 5 cases were randomly selected; one neutral, two stable and two unstable. The selected profiles were rotated such that v=0 at hub height. Figure 2 shows the profiles used.

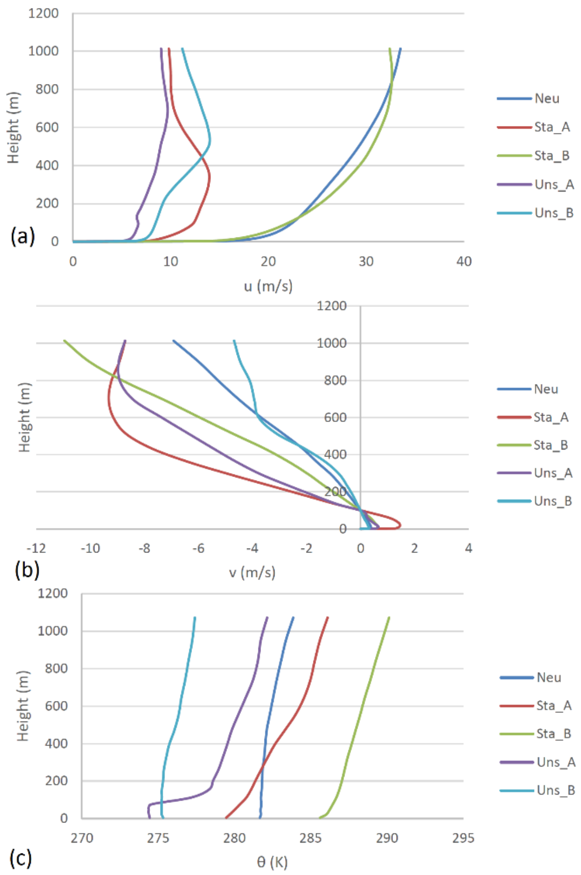

Fig 2. Forcing profiles of u (a), v (b) and potential temperature, θ (c).

4. RESULTS

Snapshots of the streamwise velocity field for the neutral case are shown in Figure 3, and in Figure 4 profiles of the horizontally averaged u and v components are shown for each of the forcing timescales.

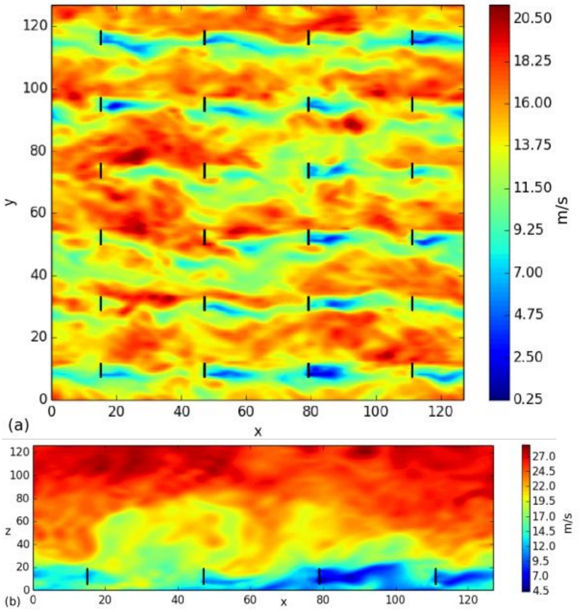

Figure 3. Snapshots of the streamwise velocity field in (a) the x-y plane at hub height, and (b) in the x-z plane through a single turbine row. Dimensions are given in grid points ($\Delta x \approx 25m$).

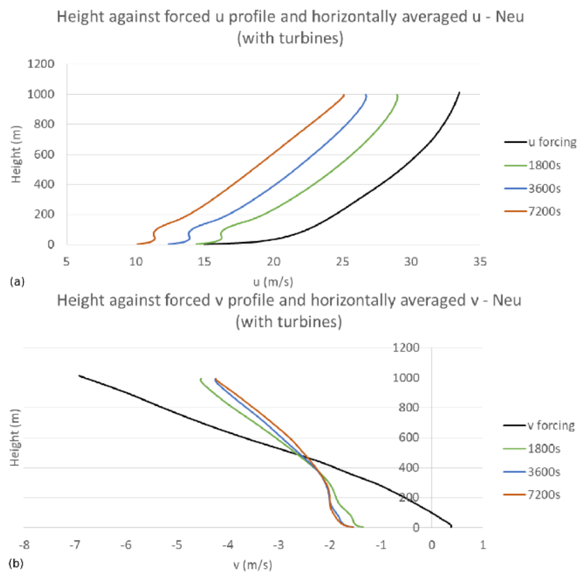

Figure 4. Horizontally averaged profiles of u (a), and v (b) for the neutral case.

From Figures 3 and 4 it can be seen the inclusion of turbines has the expected dual effects of reducing the mean flow speed due to the extraction of energy, and increasing the vertical mixing due to the production of TKE (not shown). This enhanced vertical mixing adds some additional complexity to the analysis when using realistic ABL profiles. Due to the turning of the wind with height, the momentum mixed down from aloft is veered relative to the hub height winds, hence, although v=0 in the forcing profile, this is not maintained in the presence of turbines. The effect is equivalent to a persistent yaw error in the turbine alignment. However, since only the u component is used in the calculation of U_T, U_F etc. this does not directly affect the calculation of C_P . It is, however, noticeable in the misalignment of the wakes, meaning that wake interaction effects vary between cases.

Table 2 gives the values of the key model variables calculated from the simulations together with the error with respect to the N16 model (Eq. 1). As noted in Section 3 an adjustment was necessary to account for the non-constant equivalent pressure gradient where U_{F0} and τ_{w0} are replaced by

$$\tau'_{w0} = (\langle\tau_w\rangle S + T)/S \quad (7)$$

$$U'_{F0} = U_{F0}\sqrt{\tau'_{w0}/\tau_{w0}} \quad (8)$$

The values of α, β and C_P as a function of λ/C_{f0} for both the simulated and theoretical models are shown in Figures 5-7.

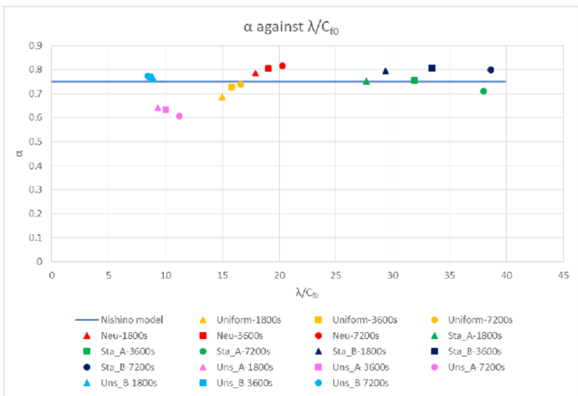

Figure 5. α as a function of $\frac{\lambda}{C_{f0}}$

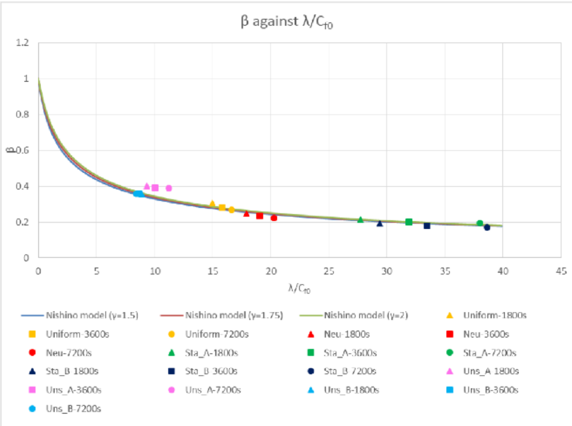

Figure 6. β as a function of λ/C_{f0}

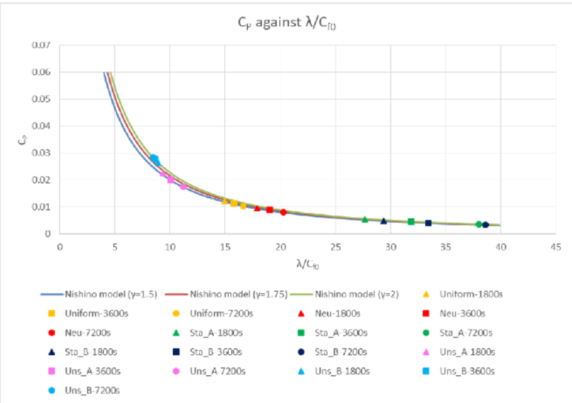

Figure 7. C_P as a function of λ/C_{f0}

For the majority of cases it can be seen from Table 2 that the N16 model does well at predicting values of α, β, and C_P, with errors typically in the region of 5%-10%. The exception to this is case uns_A, which is discussed further below. Perhaps more importantly, as shown in Figures 5-7 the N16 model also captures well the variation of α, β, and C_P as a function of λ/C_{f0}, which is important from the point of view of optimisation.

It is interesting to briefly consider the reasons behind the larger errors seen in case uns_A. In Figures 5 and 6 it can be seen that the values of α and β are over predicted and under predicted respectively by the N16 model, whereas the value of C_P is nevertheless well predicted due to the cancellation of these errors. From the definitions of α and β, this indicates that the value of the farm layer mean wind speed, U_F, is larger than assumed by the N16 model.
An underlying assumption of the N16 model is that the changes to the momentum balance within the wind farm layer are only affected by changes in surface stress combined with the thrust exerted by the turbines. However, in some circumstances the assumptions made in estimating T, and the corrections made to compensate for the forcing method may be invalid:

1) The actuator disk theory linking turbine thrust T to farm layer wind speed U_F was developed assuming a uniform flow profile and is only approximately valid in the case of a simple shear flow. For the complex shear profile found here, a correction may be necessary.
2) Unaccounted momentum added by the relaxation forcing term. Since the corrections applied in Eqs. 7 and 8 assume that the additional momentum is proportional to the stress ratio, and this may not be valid where there is a significant Reynolds-number effect on the stress ratio.

A look at the profiles for uns_A in Figs 2c and 8 show why these factors may be important.

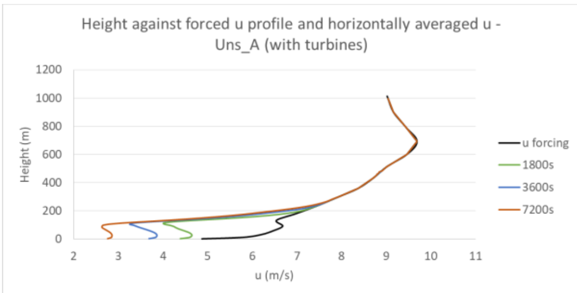

Figure 8. Streamwise velocity profiles for case uns_A.

Although the forcing profile for uns_A is classified as unstable due to a shallow layer of instability near the surface, it is also marked by a strong inversion layer in the vicinity of H_F (~210m), and a low level maximum in the wind speed close to hub height, leading to a complex shear profile throughout the wind farm layer.

5. CONCLUSIONS

The two-scale coupled momentum theory for large wind farm arrays of Nishino 2016, was tested using realistic forcing profiles in high-resolution LES simulations.

The model was found to perform well in its predictions of α, β, and C_P, with errors typically in the region of 5%-10%. In one case larger errors of around 20% were found. It was suggested that this may be due to the presence of strong velocity gradients in the vicinity of the farm layer top, H_F, and to difficulties in correcting for the forcing method used in the simulations. More work is needed to establish the precise reasons, however. In future work we propose to adapt the forcing method to allow a constant equivalent pressure gradient to be imposed whilst retaining the ability to specify the shape of the forcing profiles, since this is perhaps a more realistic representation of large-scale forcing experienced by turbine arrays.

5. REFERENCES

Brown et al. 2017. In situ data analytics for highly scalable cloud modelling on Cray machines. Concurrency Computat: Pract Exper, 30

Calaf et al. 2010 Large eddy simulation study of fully developed wind turbine array boundary layers. Phys. Fluids 22, 015110

Ghaisas et al. 2017 Farm efficiency of large wind farms. Proc. Tenth International Symposium on Turbulence and Shear Flow Phenomena, 6-9 July, Chicago, IL, USA, 6pp

Hansen, M. L. O. 2015 Aerodynamics of wind turbines, Routledge.

Nishino, T., 2016. Two-scale momentum theory for very large wind farms.. *J. Phys.: Conf. Ser.* 753

Nishino, T 2018. Generalisation of the Two Scale Momentum Theory for Coupled Wind Turbine/Farm Optimisation. Submitted to 25th National Symposium on Wind Engineering, Tokyo, 3-5 December 2018

Zapata et al.. 2017 Theoretically optimal turbine resistance in very large wind farms. J. Phys.: Conf. Ser. 854, 012051

Wind Profile	Forcing Time	From simulations					% Difference from Nishino model predictions			RMS U_T
		α	β	γ	λ/C_{f0}	C_P	α	β	C_P	
Uniform	1800	0.687	0.304	1.69	15.0	0.0121	-8.4%	8.2%	-2.8%	0.20
	3600	0.728	0.279	1.60	15.8	0.0112	-3.0%	2.8%	-1.0%	0.21
	7200	0.740	0.268	1.54	16.6	0.0103	-1.5%	1.3%	-0.5%	0.22
Neu	1800	0.785	0.245	1.53	17.9	0.0095	4.6%	-4.0%	1.3%	0.33
	3600	0.805	0.233	1.49	19.0	0.0087	7.2%	-6.1%	1.9%	0.30
	7200	0.816	0.223	1.46	20.3	0.0080	8.7%	-7.3%	2.2%	0.25
Sta_A	1800	0.753	0.212	1.78	27.7	0.0054	0.4%	-0.4%	0.1%	0.12
	3600	0.755	0.199	1.90	31.9	0.0045	0.6%	-0.6%	0.1%	0.11
	7200	0.709	0.195	2.01	38.0	0.0035	-5.5%	5.6%	-0.6%	0.09
Sta_B	1800	0.795	0.191	1.43	29.4	0.0047	6.0%	-5.2%	1.3%	0.34
	3600	0.807	0.179	1.51	33.4	0.0040	7.6%	-6.6%	1.3%	0.27
	7200	0.799	0.171	1.75	38.6	0.0034	6.4%	-5.8%	0.8%	0.24
Uns_A	1800	0.643	0.399	1.86	9.3	0.0225	-14.3%	14.0%	-6.8%	0.05
	3600	0.632	0.391	1.81	10.1	0.0201	-15.8%	15.8%	-7.4%	0.04
	7200	0.608	0.388	1.88	11.2	0.0175	-19.0%	20.0%	-8.3%	0.02
Uns_B	1800	0.761	0.355	1.97	8.9	0.0264	1.5%	-1.3%	0.6%	0.20
	3600	0.769	0.357	1.98	8.7	0.0277	2.5%	-2.1%	1.0%	0.18
	7200	0.773	0.359	1.95	8.5	0.0284	3.1%	-2.6%	1.2%	0.19

Table 2. Key model parameters from the simulations compared to the N16 model predictions.